A Letters Journal Exploring the Frontiers of Physics

April 2017

EPL, **118** (2017) 28003 www.epljournal.org
doi: 10.1209/0295-5075/118/28003

Chromatin gels are auxetic due to cooperative nucleosome assembly and disassembly dynamics

Tetsuya Yamamoto[1] and Helmut Schiessel[2]

[1] *Department of Materials Physics, Nagoya University - Furocho, Chikusa-ku, Nagoya, 464-8603, Japan*
[2] *Instituut-Lorentz for Theoretical Physics - Niels Bohrweg 2, Leiden, 2333 CA, The Netherlands*

received 30 March 2017; accepted in final form 7 June 2017
published online 23 June 2017

PACS 87.16.Sr – Chromosomes, histones
PACS 87.16.dm – Mechanical properties and rheology
PACS 87.15.Zg – Phase transitions

Abstract – We study "chromatin gels", model systems for chromatin, to theoretically predict the conditions, under which such gels show negative Poisson's ratios. A chromatin gel shows phase separation due to an instability arising from the disassembly of nucleosomes by RNA polymerases during transcription. We predict a negative Poisson's ratio near a miscibility threshold due to the cooperative assembly and disassembly of nucleosomes. The Poisson's ratio becomes more negative with an increasing number of RNAP because the disassembly rate of nucleosomes increases. In contrast, the chromatin gel shows a positive Poisson's ratio far from the miscibility threshold because the assembly of nucleosomes is arrested by the expiration of freely diffusing histone proteins.

Copyright © EPLA, 2017

Introduction. – The Poisson's ratio of many materials is positive due to their tendency to resist against volume changes [1]. Recent experiments have shown that the Poisson's ratio of the nucleus of embryonic stem (ES) cells is negative in the metastable transition state, where these cells can return to a naive pluripotent state or prime for differentiation [2]. In contrast, the nucleus of ES cells in the naive pluripotent state and of differentiated cells shows positive Poisson's ratios.

DNA is packed in the nucleus into a DNA-protein complex called chromatin [3]. The repeating unit of chromatin is the nucleosome, where DNA is wound around an octamer of histone proteins by 1.65 turns [4]. Experiments have shown that chromatin in ES cells shows fluctuations in the local nucleosome concentrations on relatively long time and length scales, analogous to critical fluctuations [5]. Whether these fluctuations were observed in the transition state or the naive pluripotent state is not clear from the experiments. In contrast, chromatin of differentiated cells shows regions of relatively large nucleosome concentration that coexist with regions of smaller nucleosome concentration, analogous to phase separation. The negative Poisson's ratio of ES cells in the transition state may reflect the critical dynamics of their chromatin structures. If this is the case, the critical chromatin dynamics in the transition state may play an important role in determining the lineage of differentiation.

In our previous studies, we have treated chromatin near the nuclear membrane as a polymer brush of DNA and predicted that the DNA brush shows phase separation due to an instability arising from the fact that nucleosomes are disassembled when they collide with RNA polymerase (RNAP) during transcription [6,7]; the local concentrations of nucleosomes decrease with increasing the transcription rate and the transcription rate, in turn, increases with decreasing the local concentrations of nucleosomes due to the excluded-volume interactions between nucleosomes and RNAP. The two-phase coexistent state is reminiscent of chromatin in differentiated cells and the critical state is reminiscent of chromatin in stem cells. A cell nucleus takes in fluid and small molecules from the cytoplasm when it is expanded [2]; the coupling between fluid motion and network deformation is the essence of gel dynamics [8]. DNA gels have been reconstituted in recent experiments [9] and we use such a gel as a model system of chromatin in the cell nucleus. Indeed, synthetic gels show a large negative Poisson's ratio near the critical point [10]. We extend our previous theory of chromatin phase separation to a gel of chromatin and calculate the Poisson's ratio of such a gel.

Our theory predicts that when a chromatin gel in a solution of histone proteins and RNAP is compressed uniaxially, it is also compressed in the other directions near the critical point on time scales longer than the time scales

of nucleosome assembly and disassembly. This is because nucleosomes are assembled cooperatively by applied stress on these longer time scales. This theory also predicts that the Poisson's ratio of the chromatin gel is negative even in the two-phase coexistent state. This contrasts the fact that the nuclei of differentiated cells show a positive Poisson's ratio [2]. This discrepancy may be caused by neglecting that chromosomes in cells are enclosed by nuclear membranes. We thus treat also a chromatin gel that is enclosed by a semipermeable membrane where the number of RNAP and histone proteins in the gel is constant. In such cases, the chromatin gel also shows a negative Poisson's ratio near the miscibility threshold because the gel has relatively large concentrations of freely diffusing histone proteins, which are necessary for the assembly of new nucleosomes. The Poisson's ratio takes more negative values with increasing number of RNAP because transcription drives the disassembly of nucleosomes and increases the concentrations of freely diffusing proteins. In contrast, far from the miscibility threshold, the gel shows a positive Poisson's ratio because most of the histone proteins are already incorporated into nucleosomes.

Model. – Here we treat a gel of DNA that is swollen in a solution of RNA polymerase and histone proteins (and other molecular machinery that is necessary for transcription and nucleosome assembly). DNA chains are modeled as 1d lattices of binding sites, which can be occupied by RNAP or nucleosomes. We derive the extension ratios $\lambda_\parallel$ and $\lambda_\perp$ of the network when stress $\Pi_{\rm app}$ is applied uniaxially, where $\lambda_\perp$ is the extension ratio in the direction of applied stress and $\lambda_\parallel$ is the extension ratio in the other (lateral) directions (see fig. 1).

The free-energy density of the chromatin gel has the form [8]

$$f_{\rm gel} = f_{\rm ela} + \frac{\phi_0}{\phi} f_{\rm sol}, \tag{1}$$

where the first and second terms are the elastic energy and the mixing free energy of the gel, respectively. Without changing the physics, we neglect the elastic energy of the nuclear membranes. This free energy is an extension of our previous model [6,7] of a chromatin brush. ϕ is the volume fraction of the DNA network after the deformation and ϕ_0 is the volume fraction in the hypothetical reference state (the state before the gel is swollen in the solution). The volume fraction ϕ is related to the extension ratios via $\phi = \phi_0/(\lambda_\parallel^2 \lambda_\perp)$. The free-energy density $f_{\rm gel}$ is thus a function of the extension ratios $\lambda_\parallel$ and $\lambda_\perp$.

In general, the elastic energy $f_{\rm ela}$ depends on the length of subchains (the chain portions between two neighboring cross-links) relative to their persistence length and on the connectivity of the network. For simplicity, we use here the neo-Hookean elastic energy [8]

$$f_{\rm ela} = \frac{1}{2} G_0 (2\lambda_\parallel^2 + \lambda_\perp^2 - 3), \tag{2}$$

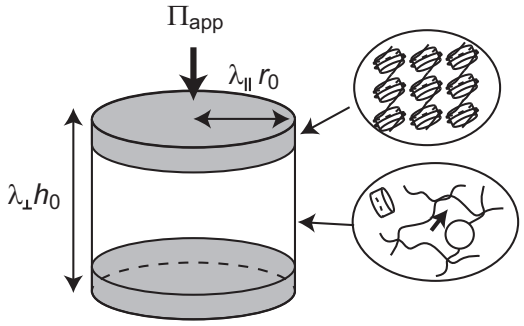

Fig. 1: Chromatin gel model. A network of DNA is swollen in a solution of RNA polymerase and histone proteins (and other small molecules that are necessary for transcription and nucleosome assembly). With applied normal stress $\Pi_{\rm app}$, the gel is deformed both in the normal and in the lateral directions with extension ratios $\lambda_\perp$ and $\lambda_\parallel$, respectively.

which represents the elastic energy of the network of (cross-linked) Gaussian chains. G_0 is the shear modulus, which is proportional to the number density of subchains and the thermal energy [8]. For simplicity, we neglect the fact that assembling nucleosomes decreases the effective length of DNA chain segments (see also sect. S1 in the Supplementary Material `Supplementarymaterial.pdf` (SM)). We assume that the relaxation time of cross-links is relatively large such that the chromatin gel acts as an elastic material on the time scale of interest; for longer time scales one needs to take into account the viscoelasticity of chromatin [11]. The mixing free energy has the form

$$f_{\rm sol} = \frac{1}{2} w_{\rm on} \Phi_{\rm on}^2 + w_{\rm int} \Phi_{\rm on} \Phi_{\rm off} + \frac{1}{2} w_{\rm off} \Phi_{\rm off}^2 + \frac{1}{3} u \Phi_{\rm on}^3, \tag{3}$$

where $\Phi_{\rm on}$ $(= n_{\rm his}\phi)$ is the local concentrations of nucleosomes and $\Phi_{\rm off}$ $(= (1 - n_{\rm his})\phi)$ is the local concentrations of vacant DNA chain segments (which are not occupied by nucleosomes). $n_{\rm his}$ is the nucleosome occupancy. The 2nd virial coefficients $w_{\rm on}$, $w_{\rm int}$, and $w_{\rm off}$ account for the (nucleosome)-(nucleosome) interactions, the (nucleosome)-(vacant segment) interactions, and the (vacant segment)-(vacant segment) interactions, respectively. The (vacant segment)-(vacant segment) interactions are repulsive interactions ($w_{\rm off} > 0$), whereas the (nucleosome)-(nucleosome) interactions are attractive interactions due to the tail bridging effect ($w_{\rm on} < 0$) [12,13]. We take also into account the 3-body interactions between nucleosomes with the 3rd virial coefficient u, which counteracts the complete collapse of the gel, see the fourth term of eq. (3). Because the fourth term is significant only when $n_{\rm his} \sim 1$, we use the approximation $u\Phi_{\rm on}^3 \simeq u\phi^3$ throughout the rest of this paper.

The occupancy $n_{\rm his}$ is determined by the dynamics of the assembly and disassembly of nucleosomes. Nucleosomes are relatively stable structures and are rarely disassembled or diffuse along DNA by thermal

fluctuations [14]. Experiments have shown that nucleosomes are disassembled when they collide with RNAP during transcription [15,16]. In this paper, we assume that collisions between RNAP and nucleosomes during transcription are the primary processes of nucleosome disassembly [6,7]. In steady state,

$$\Lambda_{\rm his} c(1-n_{\rm his}) = \zeta n_{\rm rnp} n_{\rm his}, \tag{4}$$

where the left-hand side represents the rate of nucleosome assembly and the right-hand side the rate of nucleosome disassembly. $\Lambda_{\rm his}$ is the rate constant that accounts for the assembly of nucleosomes. c is the concentration of the freely diffusing histone proteins in solution (between DNA chains in the network). The factor $1-n_{\rm his}$ reflects the fact that new nucleosomes are not assembled on binding sites that are already occupied. The rate constant ζ accounts for the disassembly of nucleosomes due to collisions with transcribing RNAP and $n_{\rm rnp}$ is the RNAP occupancy. The factor $n_{\rm rnp}n_{\rm his}$ reflects the fact that nucleosomes are disassembled only when they collide with transcribing RNAP. For simplicity, we neglect the fact that nucleosomes are composed of octamers of histone proteins, that there are four types of histones, and that the assembly of nucleosomes is usually guided by chaperones, such as NAP1. We also neglect the interactions between freely diffusing histone proteins and the DNA network because histone proteins are relatively small (see, *e.g.*, refs. [4] and [15]). Equation (4) has a form reminiscent of a detailed balance condition because each binding site takes only two states with respect to the nucleosome occupancy. However, it treats the non-equilibrium process, with which nucleosomes are disassembled by RNAP during transcription.

The RNAP occupancy $n_{\rm rnp}$ is determined by the transcription dynamics. The process of transcription starts when RNAP binds to a promoter, a non-coding DNA sequence, and changes its conformation. The enzyme then moves uni-directionally towards the terminator, another non-coding DNA sequence, where RNAP is released from the DNA molecule. The uni-directionality of the motion is due to the irreversible steps in RNA polymerization [17] and this drives the system to a non-equilibrium steady state. In steady state,

$$\Lambda_{\rm p}\rho = \xi n_{\rm rnp}(1-n_{\rm his}), \tag{5}$$

where the left-hand side represents the binding rate of RNAP to the promoter and the right-hand side the rate with which RNAP moves to the next binding site. The rate constant $\Lambda_{\rm p}$ accounts for the binding of RNAP to promoters and ρ denotes the concentration of freely diffusing RNAP in the solution (between DNA chains in the network). ξ is the rate constant that accounts for the uni-directional motion of RNAP to the next binding site. The factor $1-n_{\rm his}$ reflects the fact that RNAP cannot move to the next binding site if that site is occupied by a nucleosome. Equation (5) applies to cases in which the binding rate of RNAP is relatively small and RNAP does not show a traffic jam during transcription. We treat here a case in which the spatial orientations of the genes (which are defined by the unit vectors from the promoters to the terminators) are random so that there is no net flux in the gel [18]. With this approximation, the concentration of RNAP has the form $\rho = \rho_0 {\rm e}^{-v n_{\rm his}\phi}$, where the virial coefficient v accounts for the interactions between nucleosomes and freely diffusing RNAP in the solution and ρ_0 is the concentration of RNAP in the solution exterior to the gel. For simplicity, we neglect the interactions between RNAP and vacant DNA chain segments.

The force balance equation in the normal direction is derived by using the thermodynamic relationship $\Pi_{\rm app} = -\frac{1}{\lambda_\parallel^2}\frac{\partial f_{\rm gel}}{\partial \lambda_\perp}$ (with the occupancy $n_{\rm his}$ and the extension rate $\lambda_\parallel$ being kept constant) in the form

$$\Pi_{\rm app} = -\frac{G_0\lambda_\perp}{\lambda_\parallel^2} + \Pi_{\rm sol}(\phi). \tag{6}$$

$\Pi_{\rm sol}(\phi)$ ($\equiv \phi^2 \frac{\partial}{\partial\phi}(\frac{f_{\rm sol}(\phi)}{\phi})$) is the osmotic pressure of the gel. The force balance equation in the lateral direction follows from the thermodynamic relation $\sigma_\parallel = -\frac{1}{2\lambda_\parallel\lambda_\perp}\frac{\partial f_{\rm gel}}{\partial \lambda_\parallel}$ (with fixed occupancy $n_{\rm his}$ and fixed extension ratio $\lambda_\perp$) to be

$$\sigma_\parallel = -\frac{G_0}{\lambda_\perp} + \Pi_{\rm sol}(\phi). \tag{7}$$

We assume that no forces are applied to the side of the gel and thus $\sigma_\parallel = 0$ for cases in which the gel is uniform. Solving eqs. (6) and (7) leads to the extension ratios, $\lambda_\parallel$ and $\lambda_\perp$, as a function of the applied stress $\Pi_{\rm app}$.

Phase separation. – In the one-phase region, the form of the extension ratio $\lambda_\parallel$ is derived by using eq. (7) (with $\sigma_\parallel = 0$). Substituting this into eq. (6) leads to the applied stress $\Pi_{\rm app}$ as a function of the nucleosome occupancy $n_{\rm his}$ (see fig. 2). The nucleosome occupancy depends on a couple of dimensionless parameters, namely the rescaled rate constant η_0 ($\equiv \Lambda_{\rm p}\rho_0\zeta/(\Lambda_{\rm his}c\xi)$) and the rescaled virial coefficients, $n_\pm$ ($\equiv (-(w_{\rm int}-w_{\rm off}) \pm \sqrt{w_{\rm int}^2 - w_{\rm on}w_{\rm off}})/w$), $\tilde{v}$ ($\equiv v\phi_0/\lambda_{\rm off}^3$), and $\tilde{u}$ ($\equiv 2u\phi_0^3/(3G_0\lambda_{\rm off}^2)$), where w denotes a linear combination of the 2nd virial coefficients, $w = w_{\rm on} + w_{\rm off} - 2w_{\rm int}$, and $\lambda_{\rm off}$ the extension ratio $\lambda_{\rm off} = w_{\rm off}\phi_0^2/(2G_0)$. The transcription rate increases, relative to the rate of nucleosome assembly, with increasing the rescaled rate constant η_0.

For cases in which the rescaled rate constant η_0 is relatively large, the nucleosome occupancy $n_{\rm his}$ increases monotonically with increasing applied stress as long as the applied stress $\Pi_{\rm app}$ is smaller than a threshold value $\Pi_{\rm sp1}$, see the magenta curve in fig. 2. There are three solutions of the nucleosome occupancy for $\Pi_{\rm sp1} < \Pi_{\rm app} < \Pi_{\rm sp2}$, where two solutions are stable (shown by solid curves in fig. 2) and one solution is unstable (shown by the dotted curve in fig. 2), analogous to the van der Waals' theory of the gas-liquid phase transition. This implies that the chromatin gel shows phase separation in this stress regime.

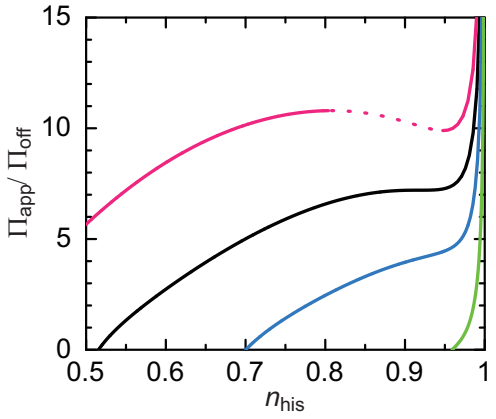

Fig. 2: (Colour online) The nucleosome occupancy n_{his} is shown as a function of applied stress Π_{app} (rescaled by Π_{off} $(= G_0/\lambda_{off})$) for cases in which the values of the rescaled rate constant η_0 are 0.05 (light green), 0.3 (blue), 0.749585 (black), and 1.5 (magenta). We used $n_+ = -1.0$, $n_- = 0.98$, $\tilde{v} = 0.8$, and $\tilde{u} = 0.01$ for the calculations. The solid curves show stable solutions and the dotted curve shows an unstable solution.

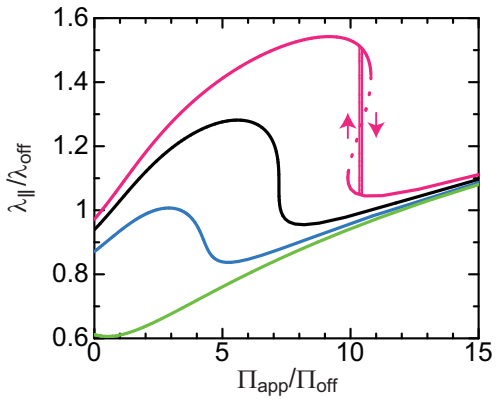

Fig. 3: (Colour online) The lateral extension ratio $\lambda_{\parallel}$ (rescaled by λ_{off}) is shown as a function of applied stress Π_{app} (rescaled by Π_{off} $(= G_0/\lambda_{off})$) for cases in which the values of the rescaled rate constant η_0 are 0.05 (light green), 0.3 (blue), 0.749585 (black), and 1.5 (magenta). We used $n_+ = -1.0$, $n_- = 0.98$, $\tilde{v} = 0.8$, and $\tilde{u} = 0.01$ for the calculations. The solid curves show stable solutions and the dotted curve shows an unstable solution.

The two threshold stresses, Π_{sp1} and Π_{sp2}, thus define the spinodal curve. When the applied stress Π_{app} is larger than the second threshold value Π_{sp2}, the nucleosome occupancy again increases monotonically with increasing applied stress. The difference $\Pi_{sp2} - \Pi_{sp1}$ between the two threshold stresses decreases with decreasing the rescaled rate constant η_0 and eventually becomes zero at the critical rescaled rate constant η_{0c} (see the black curve in fig. 2). For $\eta_0 < \eta_{0c}$, the nucleosome occupancy increases monotonically with increasing applied stress (see the blue and light green curves in fig. 2). Our theory predicts that the chromatin structure changes from the critical state to the two-phase coexistent state by increasing the rescaled rate constant η_0 and the applied stress Π_{app}, reminiscent of the differentiation of stem cells.

We use the Maxwell construction to derive the condition under which the swollen phase (that has a smaller nucleosome occupancy) coexists with the collapsed phase (that has a larger nucleosome occupancy). This condition ensures that the work that is necessary to change a small portion of the swollen phase to the collapsed phase is zero:

$$\int_{\lambda_\perp^s}^{\lambda_\perp^c} \mathrm{d}\lambda_\perp \left[-\frac{G_0 \lambda_\perp}{\lambda_\parallel^2} + \Pi_{sol}(\phi) - \Pi_{app} \right] = 0, \qquad (8)$$

where the superscripts ^{s} and ^{c} indicate the values of the parameters in the swollen and collapsed phases, respectively. We have used this treatment before to predict the phase separation of chromatin brushes [6,7]. The lateral extension ratio $\lambda_\parallel$ is continuous at the interface between the two phases because these two phases are elastically coupled [19,20]. For simplicity, we assume that the lateral extension ratio $\lambda_\parallel$ does not depend on the position and is determined by the condition $\sigma_\parallel^s \lambda_\parallel \lambda_\perp^s \psi + \sigma_\parallel^c \lambda_\parallel \lambda_\perp^c (1-\psi) = 0$, where ψ is the fraction of DNA chains in the swollen phase. This treatment is exact for cases in which the thickness of one or both of the phases is very small [20]. We perform the integration of eq. (8) by fixing the lateral extension ratio $\lambda_\parallel$ to a constant value (see also sect. S2 in the SM).

For all cases, the normal extension ratio $\lambda_\perp$ decreases with increasing applied stress Π_{app} (see fig. S1 in the SM). Thus, the Poisson's ratio of the gel is negative (positive) when the lateral extension ratio decreases (increases) with increasing applied stress. For time scales longer than the time scales of nucleosome assembly and disassembly, the lateral extension ratio decreases with increasing applied stress in a small range of intermediate values even for $\eta_0 < \eta_{0c}$, see the blue curve in fig. 3. The slope of the lateral extension becomes more negative with increasing the rescaled rate constant η_0 and diverges at the critical value η_{0c}, see the black curve in fig. 3. This is because nucleosomes are assembled cooperatively with a small increase of the applied stress in this stress regime, see also fig. 2. For $\eta_0 > \eta_{0c}$, the lateral extension ratio jumps at the threshold pressure, at which swollen and collapsed phases coexist. The threshold pressure is slightly larger for the case of increasing applied stress than for the case of decreasing applied stress [19,20]. The jump of the lateral extension ratio implies that the chromatin gel shows a very large negative Poisson's ratio in the two-phase coexistent state. This is in contrast to the fact that the nuclei of differentiated cells, which have two coexisting chromatin regions, show a positive Poisson's ratio. Our results imply that the negative Poisson's ratio is rather a generic property of chromatin gels because nucleosomes are assembled or disassembled cooperatively near the critical point and in the two-phase coexistent state.

When a small stress is superimposed to the applied stress Π_{app} for a time period shorter than the time scales

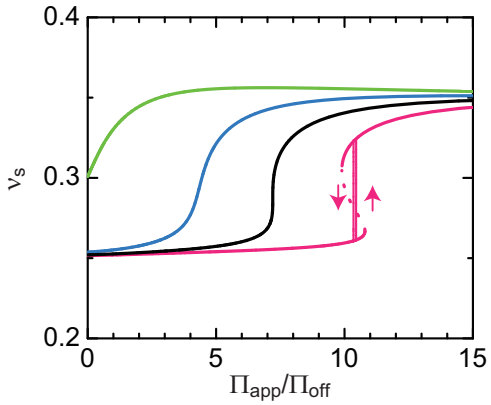

Fig. 4: (Colour online) The Poisson ratio of the deformation generated by the small stress, which is superimposed to the applied stress for a short period of time, is shown as a function of applied stress Π_{app} (rescaled by Π_{off} $(= G_0/\lambda_{off})$). We calculated for cases in which the values of the rescaled rate constant η_0 are 0.05 (light green), 0.3 (blue), 0.749585 (black), and 1.5 (magenta). We used $n_+ = -1.0$, $n_- = 0.98$, $\tilde{v} = 0.8$, and $\tilde{u} = 0.01$ for the calculations. The solid curves show stable solutions and the dotted curve shows an unstable solution.

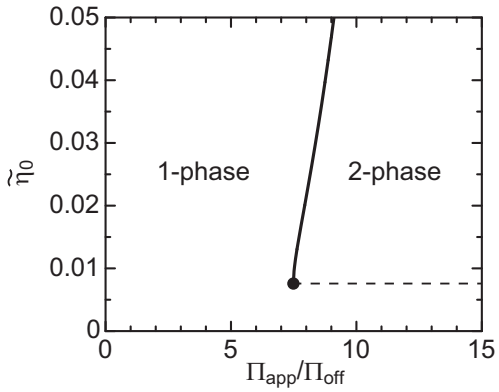

Fig. 5: The phase diagram of a chromatin gel is shown as a function of the rescaled rate constant $\tilde{\eta}_0$ and applied stress Π_{app} (rescaled by Π_{off} $(= G_0/\lambda_{off})$) for cases in which the rescaled number of histone proteins is very large $N_{his}/N_b \gg 1$. The area on left of the curve is a one-phase region and that on the right of the curve is a two-phase coexistence region. The phase boundary ends at the critical point ($\tilde{\eta}_{0c} = 0.00757894$ and $\Pi_c = 7.48738$). We used $n_+ = -0.1$, $n_- = 0.98$, $\tilde{v} = 0.8$, and $\tilde{u} = 0.01$ for the calculations.

of nucleosome assembly and disassembly, the Poisson's ratio due to the superimposed deformation has the form

$$\nu_s = \frac{1}{2}\frac{\phi\Pi'_{sol}(\phi) - \Pi_{sol}(\phi)}{\phi\Pi'_{sol}(\phi)}, \tag{9}$$

in the one-phase region (for the derivation, see sect. S3 in the SM). The Poisson's ratio in the short time scale is positive even at the critical point, see fig. 4. This result further supports our claim that the negative Poisson's ratio on long time scales is due to the cooperative assembly and disassembly of nucleosomes. Our theory predicts that the Poisson's ratio of the chromatin gel has a positive value immediately after stress is applied and then gradually decreases to a negative value. The two regimes cross over at the time scales of nucleosome assembly and disassembly.

Finite histone number. – Chromosomes in the cell nucleus are enclosed by a nuclear membrane and the number of RNAP and histone proteins may be approximately constant over time scales much shorter than the cell cycle. To mimic such a situation, we treat here a chromatin gel that is enclosed by a semipermeable membrane, which is permeable to solvent and small molecules, but not to RNAP and histone proteins. The fact that the number of RNAP and histone proteins is constant is taken into account by treating the concentrations ρ_0 and c as Lagrange multipliers. The values of these Lagrange multipliers are determined by the conditions

$$\frac{N_{rnp}}{v_b N_b} = \frac{\rho^s}{\phi^s}\psi + \frac{\rho^c}{\phi^c}(1-\psi), \tag{10}$$

$$\frac{N_{his}}{N_b} = cv_b\left(\frac{\psi}{\phi^s} + \frac{1-\psi}{\phi^c}\right) + \psi n^s_{his} + (1-\psi)n^c_{his}, \tag{11}$$

where N_{rnp} is the number of RNAP and N_{his} is the number of histone proteins in the gel. v_b is the volume of DNA per binding site and N_b is the number of binding sites in the network. Equation (10) applies to cases in which the number of transcribing RNAP is relatively small. With eqs. (10) and (11) the rescaled rate constant η_0 is no longer a constant and is determined by the condition

$$\tilde{\eta}_0 = \eta_0 \frac{\psi\rho^s/\phi^s + (1-\psi)\rho^c/\phi^c}{\psi/\phi^s + (1-\psi)/\phi^c} \times \left(1 - \frac{\psi n^s_{his} + (1-\psi)n^c_{his}}{n_0}\right), \tag{12}$$

where we used parameters $\tilde{\eta}_0 = \Lambda_p\zeta N_{rnp}/(\Lambda_{his}\xi N_{his})$ and $n_0 = N_{his}/N_b$ (see sect. S4 in the SM for the derivation).

In this case, the chromatin gel shows a phase separation for applied stresses that are larger than a threshold value, see fig. 5. This is in contrast to the van der Waals' theory of gas-liquid phase transitions, where the gas phase coexists with the liquid phase only along the phase boundary line. The reason is that the rescaled rate constant η_0 (which corresponds to the temperature in van der Waals' theory) is no longer a control parameter, but is determined by eq. (12). The two-phase coexistence state is a solution of the force balance equations, but one cannot check whether it is the most stable state by using the free energy because the gel is not in an equilibrium state. We nevertheless show in the following the properties of the latter state.

For all cases, the normal extension ratio $\lambda_\perp$ decreases with increasing applied stress Π_{app} (see fig. S2 in the SM). The Poisson's ratio is thus negative (positive) when the lateral extension ratio $\lambda_\parallel$ decreases (increases) with increasing applied stress Π_{app}. The lateral extension ratio $\lambda_\parallel$ decreases with increasing applied stress Π_{app} near the

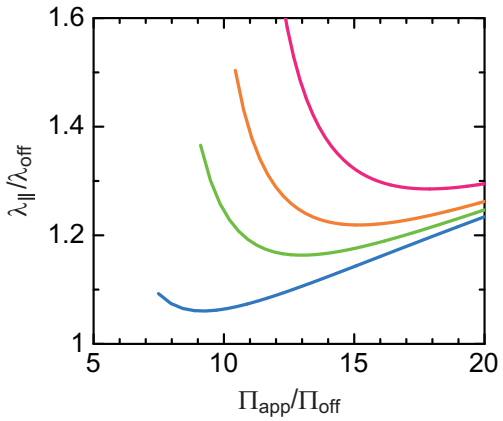

Fig. 6: (Colour online) The lateral extension ratio $\lambda_\parallel$ (rescaled by λ_{off}) is shown as a function of applied stress Π_{app} (rescaled by Π_{off} $(= G_0/\lambda_{off})$) in the two-phase coexistent state for several values of $\tilde{\eta}_0$: $\tilde{\eta}_0 = 0.00757865$ (blue), 0.05 (light green), 0.1 (orange), and 0.2 (magenta). We here show cases in which the rescaled number of histone proteins is very large, $N_{his}/N_b \gg 1$. We used $n_+ = -0.1$, $n_- = 0.98$, $\tilde{v} = 0.8$, and $\tilde{u} = 0.01$ for the calculations. Cases in which the rescaled number N_{his}/N_b of histone proteins is small are shown in fig. S3 in the SM.

miscibility threshold, see fig. 6. This is because the chromatin gel has a relatively large concentration of freely diffusing histone proteins, which are needed for the assembly of new nucleosomes. The slope of the lateral extension ratio $\lambda_\parallel$ becomes more negative with increasing number of RNAP in the gel because transcription drives the disassembly of nucleosomes and increases the concentration of freely diffusing histone proteins. The slope of the lateral extension ratio $\lambda_\parallel$ is not very large near the critical point; the criticality does not play a significant role in the negative Poisson ratio of the gel (see the blue curve in fig. 6). For larger applied stresses, the lateral extension ratio $\lambda_\parallel$ increases with increasing applied stress Π_{app}, reflecting the fact that most histone proteins in the gel are already incorporated into nucleosomes.

Discussion. – We use an extension of our previous model of chromatin brushes to theoretically predict that chromatin gels show negative Poisson's ratios for cases in which the gel is in equilibrium with RNAP and histone proteins in solution, on time scales longer than the time scales of nucleosome assembly and disassembly. This reflects the fact that nucleosomes are assembled or disassembled cooperatively near the critical point and during phase separation. For cases in which the number of RNAP and histone proteins is constant, the Poisson's ratio becomes positive far from the miscibility threshold even during phase separation. This is because most histone proteins are incorporated already into nucleosomes, which suppresses the assembly of new nucleosomes. The Poisson ratio becomes negative by increasing the number of RNAP in the gel because transcription drives the disassembly of nucleosomes and thus increases the concentrations of freely diffusing histone proteins. This prediction is relatively generic and probably does not depend on the specific model of chromatin and the disassembly process of nucleosomes. Our predictions may be experimentally accessible by using simple reconstituted systems, such as those used in ref. [9], and/or a mixture of DNA, cross-linkers, histone proteins, and RNAP enclosed in a vesicle of nuclear membrane extract.

We used a model system to find a physical principle that could relate two independent experiments, one showing that chromatin in stem cells is auxetic in the transition state [2] and the other observing critical fluctuations of the local nucleosome concentration [5]. Our theory predicts that a negative Poisson's ratio is rather a generic property of chromatin gels on long time scales. The criticality increases the negative Poisson ratio for cases in which a chromatin gel is in equilibrium with a solution of histone proteins, but it is not even significant for cases in which the number of histone proteins in the gel is constant or for time scales shorter than the time scales of the nucleosome assembly and disassembly. This is in contrast to gels of synthetic polymers, which are auxetic near the critical point [10] (however, note a theoretical prediction [21] that synthetic gels show negative Poisson's ratios even in a good solvent for a window of applied strains when they are uniform). The rate of nucleosome disassembly rather plays an important role in making the Poisson's ratio of chromatin gels negative.

Although our theory treats a model system, our theory may capture the essential features of cell nuclei. Our theory does not take into account the elasticity of nuclear membranes. Indeed, lamin A/C proteins are not expressed in stem cells and their membranes are rather flexible [5]. Because lamin A/C is not expressed both in the transient and in the naive pluripotent states [2], the elasticity of nuclear membranes probably does not play an essential role in determining the sign of the Poisson ratio of stem cells. The nuclei of stem cells show positive Poisson's ratio in the naive pluripotent state and their Poisson's ratios become negative when histone deacetylases (HDACs) are inhibited [2]. Comparison between this and our theory predicts that the inhibition of HDACs increases the rate of nucleosome disassembly. This might be the case because the deacetylation of histone tails by HDACs increases the attractive interactions between nucleosomes and stabilizes closed chromatin structures; inhibiting HDACs may make it easier for RNAP to penetrate into condensed chromatin regions and to disassemble nucleosomes.

The auxeticity of stem cell nuclei was observed in experiments on the time scale of 0.01–0.1 s [2]. The stress relaxation time of chromatin in a nucleus is on the order of 1 s [22] and thus chromatin is elastic for the time scale of the aforementioned experiments, consistent with the assumption of our theory. *In vitro* experiments have shown that the time scale of nucleosome assembly is on the order of minutes [23,24]. Our theory may suggest that chromatin of stem cells has a mechanism that accelerates the

rates of the assembly and disassembly of nucleosomes. If this is not the case, our theory predicts that the Poisson's ratio is positive even near the critical point on the time scale of the experiments in ref. [2]. Equation (9) is the generic form of the Poisson's ratio on short time scales and it predicts that the osmotic pressure plays an important role for the Poisson's ratio of chromatin on these time scales. A more detailed treatment of the interactions between nucleosomes and the effects of post-translational modification of histone tails on these interactions may elucidate the physical mechanisms involved in the negative Poisson's ratio of stem cell chromatin. Experiments that measure the Poisson's ratio of stem cell nuclei as a function of time may determine which is the case.

* * *

We acknowledge the two referees for constructive and insightful comments.

REFERENCES

[1] Greaves G. N., Greer A. L., Lakes R. S. and Rouxel T., *Nat. Mater.*, **10** (2011) 823.
[2] Pagliara S., Franze K., McClain C. R., Wylde G. W., Fisher C., Franklin R. J. M., Kabla A. J., Keyser U. F. and Chalut K. J., *Nat. Mater.*, **13** (2014) 638.
[3] Schiessel H., *J. Phys.: Condens. Matter*, **15** (2003) R699.
[4] Luger K., Mäder A. W., Richmond R. K., Sargent D. F. and Richmond T. J., *Nature*, **389** (1997) 251.
[5] Talwar S., Kumar A., Rao M., Menon G. I. and Shivashankar G. V., *Biophys. J.*, **104** (2013) 553.
[6] Yamamoto T. and Schiessel H., *Langmuir*, **32** (2016) 3036.
[7] Yamamoto T. and Schiessel H., *Transcription dynamics stabilizes nucleus-like layer structure in chromatin brush*, submitted to *Soft Matter*.
[8] Doi M., *Soft Matter Physics* (Oxford University Press, Oxford) 2013.
[9] Bertrand O. J. N., Fygenson D. K. and Saleh O. A., *Proc. Natl. Acad. Sci. U.S.A.*, **109** (2012) 17342.
[10] Hirotsu S., *J. Chem. Phys.*, **94** (1991) 3949.
[11] Bruinsma R., Grosberg A. Y., Rabin Y. and Zidovska A., *Biophys. J.*, **106** (2014) 1871.
[12] Mangenot S., Raspaud E., Tribet C., Belloni L. and Livolant F., *Eur. Phys. J. E*, **7** (2002) 221.
[13] Mühlbacher F., Holm C. and Schiessel H., *Europhys. Lett.*, **73** (2006) 135.
[14] Blossey R. and Schiessel H., *FEBS J.*, **278** (2011) 3619.
[15] Bintu L., Kopaczynska M., Hodges C., Lubkowska L., Kashlev M. and Bustamante C., *Nat. Struct. Mol. Biol.*, **18** (2011) 1394.
[16] ten Heggeler-Bodier B., Muller S., Monestier M. and Wahli W., *J. Mol. Biol.*, **299** (2000) 853.
[17] Jülicher F. and Bruinsma R., *Biophys. J.*, **74** (1998) 1169.
[18] Yamamoto T. and Safran S. A., *Soft Matter*, **11** (2015) 3017.
[19] Sekimoto K., *Phys. Rev. Lett.*, **70** (1993) 4154.
[20] Tomari T. and Doi M., *Macromolecules*, **28** (1995) 8334.
[21] Pekarski P., Tkachenko A. and Rabin Y., *Macromolecules*, **27** (1994) 7192.
[22] Celedon A., Hale C. M. and Wirtz D., *Biophys. J.*, **101** (2011) 1880.
[23] Plavner Hazan N., Tomov T. E., Tsukanov R., Liber M., Berger Y., Masoud R., Toth K., Langowski J. and Nir E., *Biophys. J.*, **109** (2015) 1676.
[24] Bennnink M. L., Leuba S. H., Leno G. H., Zlatanova J., de Grooth B. G. and Greve J., *Nat. Struct. Biol.*, **8** (2001) 606.